Simulations of GPR in Dispersive Media Using A Frequency-Dependent PSTD Algorithm

Qing Huo Liu, *Senior Member, IEEE*, and Guo-Xin Fan, *Member, IEEE*

***Abstract*— Recently an efficient pseudospectral time-domain (PSTD) algorithm has been developed to solve partial differential equations in computational electromagnetics and acoustics. It uses the fast Fourier transform (FFT) algorithm to approximate spatial derivatives, and the perfectly matched layer (PML) to eliminate the wraparound effect. Due to its high accuracy in the spatial derivatives, this method requires a significantly smaller number of unknowns than a conventional finite-difference time-domain (FDTD) method when solving large-scale problems. In this work, we further extend the PSTD algorithm to frequency-dependent media and apply the algorithm to simulate ground-penetrating radar (GPR) measurements in a dispersive earth. The dispersion of the soil is treated by the recursive convolution approaches. The convergence property of the PSTD algorithm is investigated for the scattering of a dispersive cylinder. Multidimensional large-scale problems in GPR measurements are presented to demonstrate the efficiency of this frequency-dependent PSTD algorithm.**

***Index Terms*— Dispersive media, FDTD, ground-penetrating radar (GPR), numerical analysis, pseudospectral time-domain (PSTD), perfectly matched layer (PML).**

I. Introduction

It is well known that in the frequency range of ground penetrating radar, the soil is dispersive. More specifically, the dielectric constant and conductivity of the soil are functions of frequency. This frequency dispersion of material properties can significantly affect the measurements. Failure to account for this dispersion effect will result in substantial errors in the interpretation of ground-penetrating radar (GPR) measurements.

To incorporate the dispersion of medium in the time-domain solutions, a temporal convolution of the susceptibility function and the electric field is needed. A straightforward solution of this temporal convolution requires the storage of the history of electric field, which is very inefficient because of the large memory requirement. Conventional methods proposed to tackle this problem include recursive convolution (RC) and piecewise linear recursive convolution (PLRC) [1]–[7], auxiliary differential equation (ADE) [8]–[12], and Z-transform (ZT) [13]–[15]. Here we adopt the slightly improved RC and PLRC approaches [16], [17]. It was recently found [16]–[18] that, unlike the previous results, the RC approach can be made accurate despite its piecewise constant approximation within each time step.

The finite-difference time-domain (FDTD) method [19] has been widely used together with the above approaches to simulate transient electromagnetic fields in dispersive media [1]–[18]. These frequency-dependent FDTD methods use the finite differences to approximate the spatial and temporal derivatives. As is well known, the conventional FDTD method using Yee's algorithm has the second-order accuracy both in spatial and temporal derivatives. For small- and moderate-scale problems, the FDTD method proves to be a very powerful computation tool. It has been widely used to solve time-domain problems for both nondispersive and dispersive media.

As the available computer speed and memory grow rapidly, more and more large-scale problems are being solved with time-domain methods. It is very desirable to use high-order schemes, instead of the conventional second-order FDTD method, to solve large-scale problems. Recently, a Fourier pseudospectral time-domain method combining the FFT algorithm and the PML absorber has been proposed to solve wave equations for nondispersive media [20]–[22]. The Chebyshev pseudospectral time-domain algorithm has also been used to solve scattering problems [23], [24]. In this work, we extend the multidimensional Fourier pseudospectral time-domain (PSTD) algorithm to simulate GPR measurements in dispersive media. The PML [25] is formulated for dispersive media and used to eliminate the wraparound effect in the PSTD method. Previously, the PML has been formulated both using the split and unsplit approaches for nondispersive media (e.g., [25]–[31]). Recently, these PML formulations have been further extended to dispersive media [22], [23], [33–[35]. In this work, the PML formulation in [16], [17] for general dispersive media is adopted for the PSTD algorithm. As demonstrated in [20]–[22] for nondispersive media, the PSTD method can be orders of magnitude more efficient than the FDTD method.

However, in all previous results, we have only shown the wideband signals for the total fields and scattered fields which have negligible amplitude at the high-frequency limit. Therefore, the question regarding the accuracy of the PSTD at the high-frequency limit (i.e., at the limit near the Nyquist sampling rate) remains unanswered. Here for the first time we use the normalized scattered field spectrum (i.e., the spectral ratio of the scattered field and the incident field) to answer this

Manuscript received November 3, 1998; revised May 21, 1999. This work was supported by the U.S. Environmental Protection Agency under PECASE Grant CR-825-225-01 and by the National Science Foundation under Career Grant ECS-9702195.

Q. H. Liu was with the Klipsch School of Electrical and Computer Engineering, New Mexico State University, Las Cruces, NM 88003 USA. He is now with the Department of Electrical and Computer Engineering, Duke University, Durham, NC 27707-0291 USA (e-mail: qhliu@ee.duke.edu).

G.-X. Fan is with the Klipsch School of Electrical and Computer Engineering, New Mexico State University, Las Cruces, NM 88003 USA.

Publisher Item Identifier S 0196-2892(99)06969-7.

0196–2892/99$10.00 © 1999 IEEE

question. We verify that the PSTD method can indeed allow a grid density close to the Nyquist sampling rate for narrowband signals, thus saving significant computer resources for large-scale problems.

In Section II, we summarize the PML and recursive convolution approaches for dispersive media. The frequency-dependent PSTD scheme is then presented. The validation of the PSTD algorithm is presented in Section III, followed by the applications to ground-penetrating radar measurements in large-scale inhomogeneous dispersive earth.

II. Formulation

A. PML for a General Dispersive Medium

Consider an inhomogeneous, conductive and electrically dispersive medium with magnetic permeability μ and conductivity σ. The perfectly matched layer (PML) originally proposed by Berenger [25] can be further extended to conductive and dispersive medium, as in [16], [17], [33]–[35]. Following the formulation of [16], [17] using the complex stretched coordinates [26], we can arrive at the PML modified Faraday's and Ampere's laws as

$$\frac{\partial}{\partial \eta}(\hat{\eta}\times \boldsymbol{E}) = -a_\eta \mu \frac{\partial \boldsymbol{H}^{(\eta)}}{\partial t} - \mu\omega_\eta \boldsymbol{H}^{(\eta)} - \boldsymbol{M}^{(\eta)} \tag{1}$$

$$\frac{\partial}{\partial \eta}(\hat{\eta}\times \boldsymbol{H}) = a_\eta \frac{\partial \boldsymbol{D}^{(\eta)}}{\partial t} + \omega_\eta \boldsymbol{D}^{(\eta)} + a_\eta \sigma \boldsymbol{E}^{(\eta)} + \omega_\eta \sigma \int_{-\infty}^{t} \boldsymbol{E}^{(\eta)}\, dt + \boldsymbol{J}^{(\eta)} \tag{2}$$

where the superscript $\eta = (x, y, z)$ is the split direction and a_η and ω_η are the scaling factor and the attenuation factor of PML, respectively. In the regular region of interest, $a_\eta = 1$, $\omega_\eta = 0$; while in the PML region in the η direction, $a_\eta \geq 1$ and $\omega_\eta > 0$ so that the outgoing waves will be strongly attenuated in the PML absorber without giving rise to reflections. The split field components are defined as

$$\boldsymbol{E} = \sum_{\eta=x,y,z} \left[\sum_{\substack{\zeta=x,y,z \\ \zeta\neq\eta}} \hat{\zeta} E_\zeta^{(\eta)} \right] \tag{3}$$

and similarly for $\boldsymbol{H}$ and electric and magnetic current densities $\boldsymbol{J}$ and $\boldsymbol{M}$. It is observed from (3) that there are six split field components for the electric field. Note that the PML modified Faraday's law remains the same as for a nondispersive medium [31]. All medium parameters may be space dependent for an inhomogeneous medium.

B. Recursive Convolution Approaches

The electromagnetic fields can be obtained by solving the modified Faraday's and Ampere's laws together with the constitutive equation. Noting that the constitutive relation takes the same form for all split components, we can omit the superscript (η) in the discussion on the constitutive relation. For a linear dispersive medium, the time-domain constitutive relation is

$$\boldsymbol{D}(t) = \epsilon_0 \epsilon_\infty \boldsymbol{E}(t) + \epsilon_0 \int_{-\infty}^{t} \boldsymbol{E}(\tau)\, \chi(t-\tau)\, d\tau \tag{4}$$

where ϵ_∞ is the relative dielectric constant at $\omega \to \infty$ and $\chi(t)$ is the dispersive susceptibility function whose frequency spectrum is denoted by $\tilde{\chi}(\omega)$.

The straightforward implementation of the temporal convolution in (4) is very inefficient as it requires the storage of the history of $\boldsymbol{E}$. This issue has been addressed using several different methods, including the recursive convolution and piecewise linear recursive convolution methods [1]–[7] and their improved forms [16], [17]. First, we approximate a general susceptibility function in the frequency domain as a sum of simple functions

$$\tilde{\chi}(\omega) = \sum_{q=1}^{M} \frac{\Gamma_q}{-i\omega - s_q} \tag{5}$$

where s_q and Γ_q are the complex poles and the corresponding residues, respectively. The corresponding time-domain expression is

$$\chi(t) = \sum_{q=1}^{N} \mathrm{Re}[\hat{\chi}_q(t)] = \sum_{q=1}^{N} \mathrm{Re}[R_q e^{s_q t} U(t)] \tag{6}$$

where $N = M$, $R_q = \Gamma_q$ when all s_q and Γ_q are real, and $N = M/2$ and $R_q = 2\Gamma_q$ when there are $M/2$ complex-conjugate pole pairs. The expressions of s_q and Γ_q for the commonly encountered dispersive media of Debye, Lorentz, and plasma can be easily derived [16], [17].

We now use a unified piecewise approximation for the field for $t \in [m\triangle t, (m+1)\triangle t]$:

$$\boldsymbol{E}(t) \approx \boldsymbol{E}(m+1) + K_a \frac{[\boldsymbol{E}(m+1) - \boldsymbol{E}(m)]}{\triangle t}[t - (m+1)\triangle t] \tag{7}$$

where $K_a = 0$ for recursive convolution (RC) [1]–[4] and $K_a = 1$ for piecewise linear recursive convolution (PLRC) [5]. In contrast to the previous observations, in [16]–[18] it was shown that by a proper integration the RC approach can be made nearly as accurate as the PLRC approach.

The approximation of a general susceptibility function by (5) and (6) is aimed to simplify the convolution integral in (4). To this end, we substitute (6) and (7) into (4). Then, we introduce an auxiliary function

$$\boldsymbol{\Psi}_q(n) = \sum_{m=0}^{n-1} \{[\hat{\chi}_q(0) - \hat{\xi}_q(0)]\boldsymbol{E}(n-m) + \hat{\xi}_q(0)\boldsymbol{E}(n-m-1)\} e^{s_q m \triangle t}$$

where the expressions of $\hat{\chi}_q(0)$ and $\hat{\xi}_q(0)$ are given by

$$\hat{\chi}_q(0) = \begin{cases} R_q \triangle t, & \text{for } s_q = 0; \\ \dfrac{R_q}{s_q}(e^{s_q \triangle t} - 1), & \text{for } s_q \neq 0 \end{cases} \tag{8}$$

$$\hat{\xi}_q(0) = \begin{cases} \dfrac{K_a R_q \triangle t}{2}, & \text{for } s_q = 0; \\ \dfrac{K_a R_q}{\triangle t s_q^2}[1-(1-s_q\triangle t)e^{s_q\triangle t}], & \text{for } s_q \neq 0. \end{cases} \tag{9}$$

By using (6) and (7), we can derive from (4) the following recursive relations:

$$\begin{aligned}\boldsymbol{\Psi}_q(n+1) =& [\hat{\chi}_q(0) - \hat{\xi}_q(0)]\boldsymbol{E}(n+1) + \hat{\xi}_q(0)\boldsymbol{E}(n) \\ &+ \boldsymbol{\Psi}_q(n)e^{s_q\triangle t}\end{aligned} \tag{10}$$

$$\begin{aligned}\boldsymbol{D}(n+1) =& \epsilon_0\left\{\epsilon_\infty + \sum_{q=1}^{N} \mathrm{Re}\left[\hat{\chi}_q(0) - \hat{\xi}_q(0)\right]\right\}\boldsymbol{E}(n+1) \\ &+ \epsilon_0 \sum_{q=1}^{N} \mathrm{Re}[\hat{\xi}_q(0)]\boldsymbol{E}(n) \\ &+ \epsilon_0 \sum_{p=1}^{N} \mathrm{Re}[\boldsymbol{\Psi}_q(n)e^{s_q\triangle t}].\end{aligned} \tag{11}$$

Thus, the expensive temporal convolution in (4) can be now achieved by the two recursive relations in (10) and (11).

Using the central time-differencing in (1) and (2) and making use of (10) and (11), we arrive at the temporally discretized equations for the electric and magnetic fields:

$$\begin{aligned}&\left(\frac{a_\eta}{\triangle t} + \frac{\omega_\eta}{2}\right)\boldsymbol{H}^{(\eta)}\left(n+\frac{1}{2}\right) \\ &\quad = \left(\frac{a_\eta}{\triangle t} - \frac{\omega_\eta}{2}\right)\boldsymbol{H}^{(\eta)}\left(n-\frac{1}{2}\right) \\ &\qquad - \frac{\partial}{\partial\eta}[\hat{\eta}\times\boldsymbol{E}(n)] - \boldsymbol{M}^{(\eta)}(n)\end{aligned} \tag{12}$$

$$\begin{aligned}&c_1^{(\eta)}\boldsymbol{E}^{(\eta)}(n+1) \\ &\quad = c_0^{(\eta)}\boldsymbol{E}^{(\eta)}(n) - \sigma\omega_\eta\triangle t\boldsymbol{E}_I^{(\eta)}(n) \\ &\qquad + \frac{\partial}{\partial\eta}\left[\hat{\eta}\times\boldsymbol{H}\left(n+\frac{1}{2}\right)\right] \\ &\qquad + \boldsymbol{\Phi}^{(\eta)}(n) - \boldsymbol{J}^{(\eta)}\left(n+\frac{1}{2}\right)\end{aligned} \tag{13}$$

where

$$\begin{aligned}\boldsymbol{\Phi}^{(\eta)}(n) =& \epsilon_0 \sum_{q=1}^{N} \mathrm{Re}\left\{\left[\left(\frac{a_\eta}{\triangle t}\frac{\omega_\eta}{2}\right)\right.\right. \\ &\left.\left. - \left(\frac{a_\eta}{\triangle t} + \frac{\omega_\eta}{2}\right)e^{-s_q\triangle t}\right]\boldsymbol{\Psi}_q^{(\eta)}(n)\right\}\end{aligned} \tag{14}$$

$$\boldsymbol{E}_I^{(\eta)}(n) = \boldsymbol{E}_I^{(\eta)}(n-1) + \frac{7}{8}\boldsymbol{E}^{(\eta)}(n) + \frac{1}{8}\boldsymbol{E}^{(\eta)}(n-1) \tag{15}$$

and

$$\begin{aligned}c_0^{(\eta)} =& \left(\frac{a_\eta}{\triangle t} - \frac{\omega_\eta}{2}\right)\epsilon_0\epsilon_\infty - \frac{a_\eta\sigma}{2} \\ &- \left(\frac{a_\eta}{\triangle t} + \frac{\omega_\eta}{2}\right)\epsilon_0\sum_{q=1}^{N}\mathrm{Re}[\hat{\xi}_q(0)]\end{aligned} \tag{16}$$

$$\begin{aligned}c_1^{(\eta)} =& \frac{\sigma}{2}\left[a_\eta + \frac{\omega_\eta\triangle t}{4}\right] + \left(\frac{a_\eta}{\triangle t} + \frac{\omega_\eta}{2}\right)\epsilon_0 \\ &\cdot\left\{\epsilon_\infty + \sum_{q=1}^{N}\mathrm{Re}[\hat{\chi}_q(0) - \hat{\xi}_q(0)]\right\}.\end{aligned} \tag{17}$$

Equations (12) and (13) form a leap-frog system. In the above, we discuss only the temporal discretization using the central differencing and recursive convolution approaches. The spatial discretization using the pseudospectral method will be discussed in the next subsection.

For GPR measurements, the dispersion of soil has to be accounted for. This dispersion is mainly caused by the presence of moisture in the soil. A common model for soil is the Debye medium whose susceptibility function is given by

$$\chi(\omega) = (\epsilon_s - \epsilon_\infty)\sum_{q=1}^{N}\frac{G_q}{1-i\omega\tau_q} \tag{18}$$

where ϵ_s is the relative static permittivity, τ_q is the Debye relaxation time constant, and G_q is the pole amplitude. The Debye medium can be considered a special case of the general equation (5) with

$$R_q = \frac{(\epsilon_s - \epsilon_\infty)G_q}{\tau_q}, \qquad s_q = -\frac{1}{\tau_q}. \tag{19}$$

Therefore, given (19) for an arbitrary Debye medium, (12) and (13) can be solved efficiently without the expensive temporal convolution.

C. The PSTD Algorithm for Dispersive Media

We now turn to the spatial discretization of (12) and (13). Traditionally, this is accomplished by the FDTD method [1]–[18] through an Yee grid [19]. In the PSTD algorithm [20]–[22], instead of using a conventional Yee grid, we use a centered grid where all field components and material properties are located at the center of the unit cell of size $\Delta x \times \Delta y \times \Delta z$. The truncated space is discretized into $N_x \times N_y \times N_z$ cells. Spatial derivatives are approximated by FFT's instead of finite differences. Thus, in the PSTD algorithm for dispersive media, we have the following leap-frog system from (12) and (13):

$$\begin{aligned}&\left(\frac{a_\eta}{\triangle t} + \frac{\omega_\eta}{2}\right)\boldsymbol{H}^{(\eta)}\left(n+\frac{1}{2}\right) \\ &\quad = \left(\frac{a_\eta}{\triangle t} - \frac{\omega_\eta}{2}\right)\boldsymbol{H}^{(\eta)}\left(n-\frac{1}{2}\right) \\ &\qquad - \mathcal{F}_\eta^{-1}\{ik_\eta\mathcal{F}_\eta[\hat{\eta}\times\boldsymbol{E}(n)]\} - \boldsymbol{M}^{(\eta)}(n)\end{aligned} \tag{20}$$

$$\begin{aligned}&c_1^{(\eta)}\boldsymbol{E}^{(\eta)}(n+1) \\ &\quad = c_0^{(\eta)}\boldsymbol{E}^{(\eta)}(n) - \sigma\omega_\eta\triangle t\boldsymbol{E}_I^{(\eta)}(n) \\ &\qquad + \mathcal{F}_\eta^{-1}\left\{ik_\eta\mathcal{F}_\eta[\hat{\eta}\times\boldsymbol{H}\left(n+\frac{1}{2}\right)]\right\} \\ &\qquad + \boldsymbol{\Phi}^{(\eta)}(n) - \boldsymbol{J}^{(\eta)}\left(n+\frac{1}{2}\right).\end{aligned} \tag{21}$$

In these equations, $\mathcal{F}_\eta$ and $\mathcal{F}_\eta^{-1}$ denote the one-dimensional (1-D) forward and inverse FFT, respectively, and k_η is the Fourier variable in the η direction. This treatment of spatial derivatives is exact up to the Nyquist sampling density, significantly reducing the number of unknowns [20]–[22].

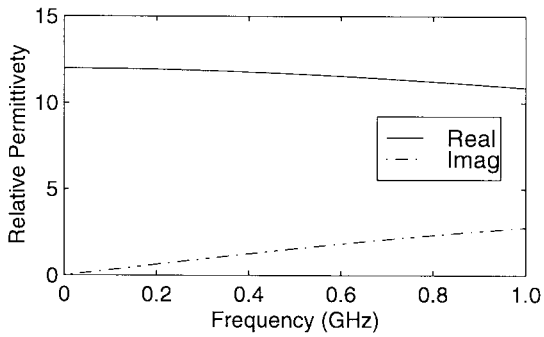

(a)

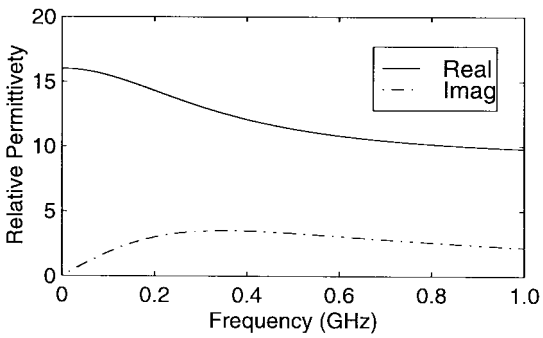

(b)

Fig. 1. Real and imaginary parts of the relative permittivity of (a) Debye medium I and (b) medium II.

TABLE I
PARAMETERS FOR DEBYE MEDIA I AND II

Medium I	Medium II
$\epsilon_\infty = 4$, $\epsilon_s = 12$ $\sigma = 0.002$ S/m $\tau = 2.0 \times 10^{-10}$ s	$\epsilon_\infty = 9$, $\epsilon_s = 16$ $\sigma = 0.004$ S/m $\tau = 6.4 \times 10^{-11}$ s
$\Gamma_1 = 40 \times 10^9$ rad/s $s_1 = -5.0 \times 10^9$ rad/s	$\Gamma_1 = 109.37 \times 10^9$ rad/s $s_1 = -15.625 \times 10^9$ rad/s

III. NUMERICAL RESULTS

To illustrate the applications of the PSTD algorithm for GPR measurements in the dispersive earth, we model two different Debye media. Fig. 1(a) and (b) displays the dispersion curves for the real and imaginary parts of the complex permittivity in mediums I and II, respectively, to be studied in the following examples. These Debye media have substantial dispersion over the frequency band of the source. The parameters for the Debye media are listed in Table I.

First we validate the three-dimensional (3-D) PSTD results for a homogeneous dispersive medium II as listed in Table I. An electric dipole oriented in x direction is located at the origin. The time function of this source is the first derivative of the Blackman-Harris window function [31] with a center frequency $f_c = 300$ MHz. The discretization is $\Delta x = \Delta y = \Delta z = 3.906\,25$ cm, and $\Delta t = 50$ ps. Fig. 2 shows the PSTD and analytical results for the E_x component at the observation point $\boldsymbol{r} = (11\Delta x, 0, 20\Delta z)$. It confirms the high accuracy of the PSTD algorithm even at this coarse grid corresponding to only 2.56 cells per wavelength at the highest frequency $f_{\max} = 2.5 f_c$.

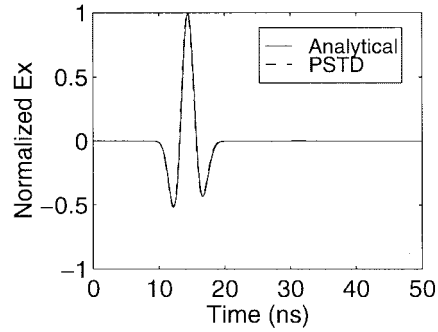

Fig. 2. Comparison of PSTD results and analytical solutions for a source in Debye medium II.

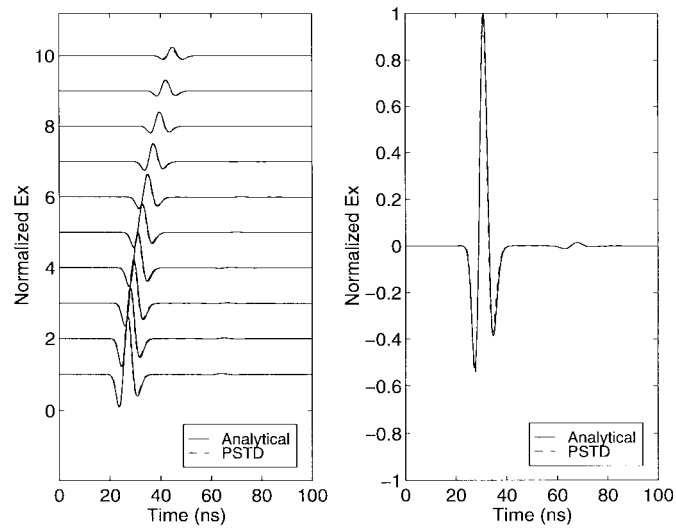

(a) (b)

Fig. 3. A sphere (Debye medium I) in Debye medium II. (a) E_x at the array of receivers. (b) E_x at the fourth receiver.

We now compare the PSTD results with analytical solutions for a dispersive sphere (medium I) embedded in the dispersive medium II. The sphere has a radius of 1.6 m. The same dipole source is now located at the center of the sphere (also the origin). The cell size is slightly increased to $\Delta x = \Delta y = \Delta z = 5$ cm, and $\Delta t = 50$ ps. Fig. 3 shows the PSTD and analytical results for the E_x component at an array of receiver locations $\boldsymbol{r} = [5(j+1)\Delta x, 0, 40\Delta z]$ $(j = 1, \cdots, 10)$, and at the fourth receiver $(j = 4)$. Note that both the direct and reflected fields agree well between the PSTD and analytical results. Note that is this case the coarse grid has a only two cells per wavelength at the highest frequency $f_{\max} = 2.5 f_c$.

However, the above results are for broadband excitations as for the nondispersive media in [20]–[22]. Therefore, the accuracy of those PSTD results is undoubtedly helped by the fact that the source excitation has negligible energy near the highest frequency $f_{\max} = 2.5 f_c$. Thus an important question arises regarding the accuracy of PSTD results under a monochromatic excitation. To answer this question, we can study the behavior of the relative scattered field (normalized by the incident field spectrum) as a function of frequency.

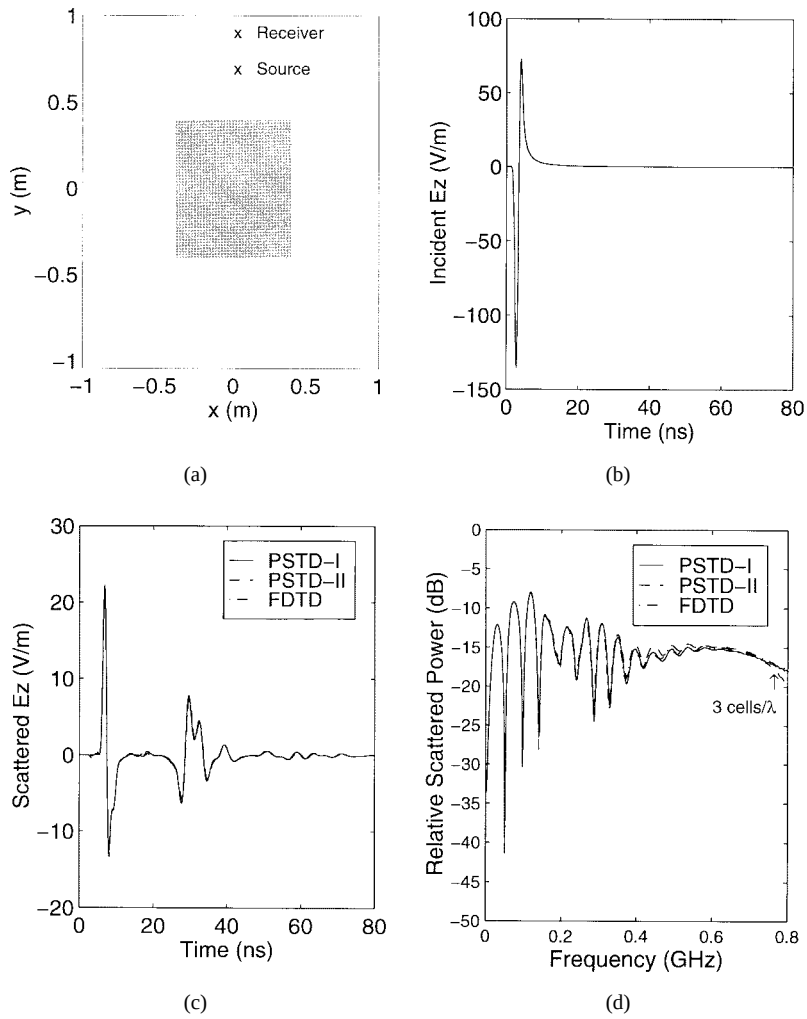

Fig. 4. Scattering by a dispersive square cylinder. (a) Geometry. (b) Incident field $E_z^{\rm inc}$ as a function of time. (c) Scattered field $E_z^{\rm sct}$ as a function of time. (d) Relative scattered power spectral amplitude $P = 20\log_{10}|\ E_z^{\rm sct}(f)/E_z^{\rm inc}(f)\ |$.

This is a more objective assessment of the accuracy of the PSTD algorithm as the accuracy is no longer helped by the low excitation energy at the high-frequency limit.

For this purpose, we compare the PSTD and FDTD results for the scattered field from a dispersive square cylinder. The cylinder is Debye medium II, and the background medium is a nondispersive medium with $\epsilon_r = 4$ and $\sigma = 0$. The geometry of the cylinder and the locations of the source and receiver are shown in Fig. 4(a). We perform the following three different simulations.

1) The PSTD with a fine grid with $\Delta x = \Delta y = 0.8$ cm and $\Delta t = 7.5$ ps.
2) The FDTD with the same discretization as 1).
3) The PSTD with a coarse grid with $\Delta x = \Delta y = 4$ cm and $\Delta t = 15$ ps.

These simulations are denoted as PSTD-I, FDTD, and PSTD-II, respectively. Note that for this particular problem, the FDTD requires 25 times more memory than PSTD-II. The source is an electric line source in z direction (J_z), and the source time function is a Gaussian pulse. Fig. 4(b) shows the incident field $E_z^{\rm inc}$ as a function of time in the absence of the square cylinder. When the dispersive cylinder is present, we calculate the total field. By subtracting the incident field in Fig. 4(b) from the total field, we obtain the scattered field $E_z^{\rm sct}$ as a function of time in Fig. 4(c). Again note that for this broadband excitation, the scattered fields from all three simulations have excellent agreement. In order to remove the frequency effect of the excitation, we normalize the scattered field spectrum by the incident field spectrum. We define the relative scattered power spectrum as

$$P(\omega) = 20\ \log_{10}\left|\frac{E_z^{\rm sct}(\omega)}{E_z^{\rm inc}(\omega)}\right|.$$

As shown in Fig. 4(d), the relative scattered power spectral amplitudes for the three simulations have excellent agreement up to the frequency $f = 0.75$ GHz. At this frequency, the grid in PSTD-II corresponds to 3 cells per wavelength, in contrast to 15 cells per wavelength in the PSTD-I and FDTD simulations. Therefore, for this medium-scale problem, the computer memory for the PSTD method is only 1/25 of that require by the FDTD method. Note if the scale of the problem increases, the required grid density (number of cells per wavelength) in the FDTD method has to be increased, while that in the PSTD algorithm remains the same. Consequently,

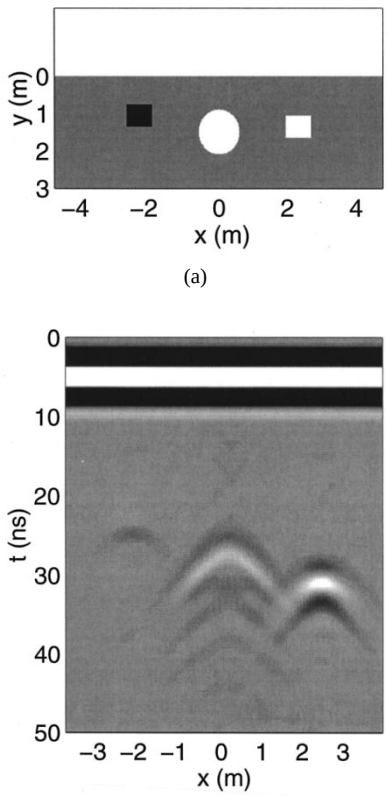

Fig. 5. (a) Geometry of three objects buried in a dispersive earth and (b) the GPR measured field.

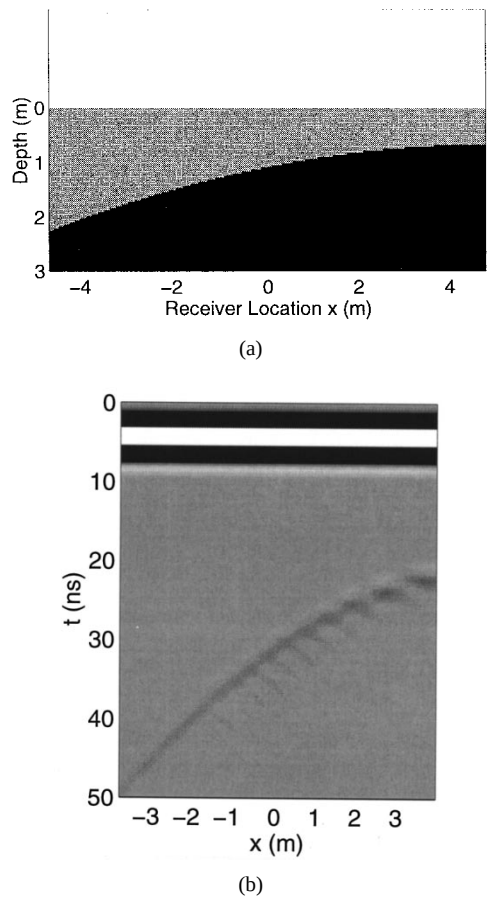

Fig. 6. (a) Layered dispersive earth with a dipping interface and (b) the GPR measured field (the direct field is saturated).

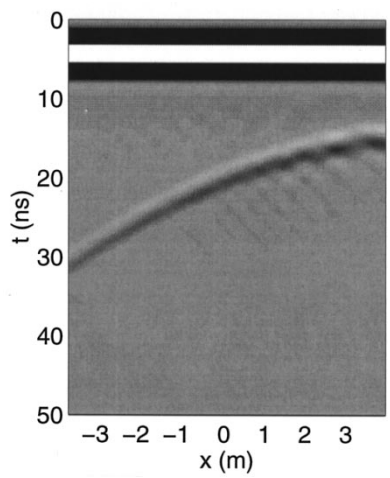

Fig. 7. Same as Fig. 6 except for the nondispersive media with $\epsilon_r = \epsilon_\infty$.

for large-scale 3-D problems, the PSTD algorithm can be orders of magnitude more efficient than the FDTD method.

As the required cell size in the PSTD algorithm can be made large without sacrificing its accuracy, this algorithm is ideal for large-scale problems in GPR applications. Fig. 5(a) shows a two-dimensional (2-D) GPR measurement configuration for the detection of objects buried in a dispersive earth (Debye medium I). The rectangular object on the left is dispersive (Debye medium II). The other two anomalies are air voids. Fig. 5(b) displays the monostatic GPR measurements on the surface with an operating center frequency of 200 MHz. It clearly shows the three buried objects. This 2-D problem is simulated by 128 $\times$ 64 cells with $\Delta x = \Delta y = 7.5$ cm and $\Delta t = 20$ ps. In contrast, a simulation by the FDTD method requires a grid of 640 $\times$ 320 in order to achieve a comparable accuracy. Therefore, for this 2-D problem, the PSTD requires a computer memory 1/25 the size of the FDTD method. The saving factor in computer time is roughly the same.

Another GPR application is to map subsurface layer interfaces. Fig. 6(a) illustrates such an example with two dispersive layers below the surface (top layer: Debye medium I; bottom layer: Debye medium II). The discretization is the same as for the last example. The monostatic GPR measurements in Fig. 6(b) clearly show the reflection from the layer interface.

To illustrate the effects of dispersion on the GPR measurements, we simulate the last problem with nondispersive media. The configuration is exactly the same as in the last example, except that the dielectric constants take the high-frequency $(\omega \to \infty)$ values of the corresponding curves in Table I. Fig. 7 displays the grey-level monostatic GPR measurements of the nondispersive media. In addition to substantial differences in the waveforms from Fig. 6(b), significant deviations in the arrival times of the reflected signals are observed. Failure to account for the medium dispersion can thus result in large errors. One may always choose another set of nondispersive medium parameters to mimic the move-out of Fig. 6(b), but

is unlikely to reproduce the same waveforms without taking the dispersion into account.

A comment on the CPU time saving for the PSTD algorithm is now in order. From our implementation of the PSTD and FDTD methods, for a typical 3-D problem with 64 $\times$ 64 $\times$ 64 cells, one time step takes 5.68 CPU s for the PSTD, and 5.43 CPU s for the FDTD, roughly about the same CPU time for the two methods. The reason for the PSTD method to perform so well is that in each 1-D forward/inverse FFT calculation it gives the spatial derivative for a whole row of data. As discussed in [20], for the same problem with a fixed physical dimension, the FDTD method requires $(KN)^D$ cells if the PSTD requires only N^D cells (D is the dimensionality). Therefore, given the same time discretization, the FDTD method requires K^D times more CPU time than the PSTD method. For the examples shown here, $K \geq 4$ and it increases with the scale of the problem. Furthermore, the program structure of the PSTD algorithm remains the same as the FDTD method except that the spatial finite differences are now replaced by a 1-D forward/inverse FFT pair.

Finally, we note that one limitation of the current PSTD algorithm is the uniform grid required by the FFT algorithm. Recently progress has been made toward the nonuniform fast Fourier transform (NUFFT) algorithms which only require $O(N \log_2 N)$ arithmetic operations [36], [37]. In the near future we hope to report the progress to incorporate these algorithms in the PSTD so that it can admit a nonuniform grid.

IV. Conclusions

We have developed a pseudospectral time-domain (PSTD) algorithm for general dispersive media. In this algorithm, an arbitrary dispersive medium is modeled by the sum of functions with simple poles, and temporal convolution integrals are simplified by improved recursive convolution (RC) and piecewise linear recursive convolution (PLRC). The fast Fourier transform (FFT) algorithm is used to approximate spatial derivatives, while the PML is used to eliminate the wraparound effects. As a result of the spectral representation of spatial derivatives, a coarse sampling close to the Nyquist density becomes possible while maintaining the accuracy. This is now verified by the normalized scattered field in the frequency domain. The algorithm has been applied to simulate GPR measurements. Future work will address the nonuniform sampling in space to make the algorithm more flexible.

References

[1] R. Luebbers, F. P. Hunsberger, K. Kunz, R. Standler, and M. Schneider, "A frequency-dependent finite difference time domain formulation for dispersive materials," *IEEE Trans. Electromagn. Compat.*, vol. 32, pp. 222–227, 1990.

[2] R. J. Luebbers, F. P. Hunsberger, and K. Kunz, "A frequency-dependent finite-difference time-domain formulation for transient propagation in plasma," *IEEE Trans. Antennas Propagat.*, vol. 39, pp. 29–39, 1991.

[3] R. J. Luebbers and F. P. Hunsberger, "FDTD for Nth-order dispersive media," *IEEE Trans. Antennas Propagat.*, vol. 40, pp. 1297–1301, 1992.

[4] R. J. Luebbers, D. Steich, and K. Kunz, "FDTD calculation of scattering from frequency-dependent materials," *IEEE Trans. Antennas Propagat.*, vol. 41, pp. 1249–1257, 1993.

[5] D. F. Kelley and R. J. Luebbers, "Piecewise linear recursive convolution for dispersive media using FDTD," *IEEE Trans. Antennas Propagat.*, vol. 44, pp. 792–797, 1996.

[6] M. D. Bui, S. S. Stuchly, and G. I. Costache, "Propagation of transients in dispersive dielectric media," *IEEE Trans. Microwave Theory Tech.*, vol. 39, pp. 1165–1171, 1991.

[7] J. M. Bourgeois and G. S. Smith, "A full three-dimensional simulation of a ground-penetrating radar: FDTD theory compared with experiment," *IEEE Trans. Geosci. Remote Sensing*, vol. 34, pp. 36–44, Jan. 1996.

[8] T. Kashiwa and I. Fukai, "A treatment by FDTD method of dispersive characteristics associated with electronic polarization," *Microw. Opt. Tech. Lett.*, vol. 3, pp. 203–205, 1990.

[9] R. M. Joseph, S. C. Hagness, and A. Taflove, "Direct time integration of Maxwell's equations in linear dispersive media with absorption for scattering and propagation of femtosecond electromagnetic pulse," *Opt. Lett.*, vol. 16, pp. 1412–1414, 1991.

[10] O. P. Gandhi, B.-Q. Gao, and J.-Y. Chen, "A frequency-dependent finite-difference time-domain formulation for general dispersive media," *IEEE Trans. Microwave Theory Tech.*, vol. 41, pp. 658–664, 1993.

[11] J. L. Young, "Propagation in linear dispersive media: Finite difference time-domain methodologies," *IEEE Trans. Antennas Propagat.*, vol. 43, pp. 422–426, 1995.

[12] A. Taflove, *Computational Electromagnetics: The Finite-Difference Time-Domain Method*. Boston, MA: Artech House, 1995.

[13] D. M. Sullivan, "Frequency-dependent FDTD methods using Z transforms," *IEEE Trans. Antennas Propagat.*, vol. 40, pp. 1223–1230, 1992.

[14] ——, "Z-transform theory and the FDTD method," *IEEE Trans. Antennas Propagat.*, vol. 44, pp. 28–34, Jan. 1996.

[15] W. H. Weedon and C. M. Rappaport, "A general method for FDTD modeling of wave propagation in arbitrary frequency-dispersive media," *IEEE Trans. Antennas Propagat.*, vol. 45, pp. 401–410, 1997.

[16] G.-X. Fan, and Q. H. Liu, "A PML-FDTD algorithm for general dispersive media," in *Proc. ACES 14th Ann. Review Progress Applied Computational Electromagnetics*, Monterey, CA, 1998, pp. 655–662.

[17] G.-X. Fan and Q. H. Liu, "A PML-FDTD algorithm for simulating plasma-covered cavity-backed slot antennas," *Microw. Opt. Tech. Lett.*, vol. 19, no. 4, pp. 258–262, 1998.

[18] J. W. Schuster and R. J. Luebbers, "An accurate FDTD algorithm for dispersive media using a piecewise constant recursive convolution technique," *IEEE Antennas Propagat. Soc. Int. Symp.*, Atlanta, GA, June 1998, pp. 2018–2021.

[19] K. S. Yee, "Numerical solution of initial boundary value problems involving Maxwell's equations in isotropic media," *IEEE Trans. Antennas Propagat.*, vol. AP-14, pp. 302–307, 1966.

[20] Q. H. Liu, "The PSTD algorithm: a time-domain method requiring only two cells per wavelength," *Microw. Opt. Tech. Lett.*, vol. 15, no. 3, pp. 158–165, 1997.

[21] ——, "The PSTD algorithm for acoustic waves in inhomogeneous, absorptive media," *IEEE Trans. Ultrason., Ferroelect., Freq. Contr.*, vol. 45, pp. 1044–1055, 1998.

[22] ——, "Large-scale simulations of electromagnetic and acoustic measurements using the pseudospectral time-domain (PSTD) algorithm," *IEEE Trans. Geosci. Remote Sensing*, vol. 37, pp. 917–926, Mar. 1999.

[23] B. Yang, D. Gottlieb, and J. S. Hesthaven, "On the use of PML ABC's in spectral time-domain simulations of electromagnetic scattering," in *Proc. ACES 13th Annu. Review Progress Applied Computational Electromagnetics*, Monterey, CA, 1997, pp. 926–933.

[24] ——, "Spectral simulations of electromagnetic waves scattering," *J. Comput. Phys.*, vol. 134, pp. 216–230, 1997.

[25] J. R. Berenger, "A perfectly matched layer for the absorption of electromagnetic waves," *J. Comput. Phys.*, vol. 114, pp. 185–200, 1994.

[26] W. C. Chew, and W. H. Weedon, "A 3D perfectly matched medium from modified Maxwell's equations with stretched coordinates," *Microw. Opt. Tech. Lett.*, vol. 7, pp. 599–604, 1994.

[27] Z. S. Sacks, D. M. Kingsland, R. Lee, and J. -F. Lee, "A perfectly matched anisotropic absorber for use as an absorbing condition,"*IEEE Trans. Antennas Propagat.*, vol. 43, pp. 1460–1463, 1995.

[28] L. Zhao, A. C. Cangellaris, "A general approach for the development of unsplit-field time-domain implementations of perfectly matched layers for FDTD grid truncation," *IEEE Microwave Guided Wave Lett.*, vol. 6, pp. 209–211, 1996.

[29] J. Fang and Z. Wu, "Generalized perfectly matched layer for the absorption of propagating and evanescent waves in lossless and lossy media," *IEEE Trans. Microwave Theory Tech.*, vol. 44, pp. 2216–2222, 1996.

[30] S. D. Gedney, "An anisotropic perfectly matched layer-absorbing medium for the truncation of FDTD lattices," *IEEE Trans. Antennas Propagat.*, vol. 46, pp. 1630–1639, 1996.

[31] Q. H. Liu, "An FDTD algorithm with perfectly matched layers for conductive media," *Microw. Opt. Tech. Lett.*, vol. 14, pp. 134–137, 1997.

[32] R. W. Ziolkowski, "Time-derivative Lorentz material model-based absorbing boundary condition," *IEEE Trans. Antennas Propagat.*, vol. 45, pp. 1530–1535, 1997.
[33] S. D. Gedney, "An anisotropic PML absorbing media for the FDTD simulation of fields in lossy and dispersive media," *Electromagnetics*, vol. 16, pp. 399–415, 1996.
[34] T. Uno, Y. He, and S. Adachi, "Perfectly matched layer absorbing condition for dispersive medium," *IEEE Microwave Guided Wave Lett.*, vol. 7, pp. 264–266, 1997.
[35] F. L. Teixeira, W. C. Chew, M. Straka, M. L. Oristaglio, and T. Wang, "Finite-difference time-domain simulation of ground penetrating radar on dispersive, inhomogeneous, and conductive soils," *IEEE Trans. Geosci. Remote Sensing*, vol. 36, pp. 1928–1937, 1998.
[36] Q. H. Liu, and N. Nguyen, "An accurate algorithm for nonuniform fast Fourier transforms (NUFFT)," *IEEE Microwave Guided Wave Lett.*, vol. 8, pp. 18–20, Jan. 1998.
[37] Q. H. Liu, and X. Y. Tang, "An iterative algorithm for nonuniform inverse fast Fourier transform (NU-IFFT)," *Electron. Lett.*, vol. 34, no. 20, pp. 1913–1914, 1998.

Qing Huo Liu (S'88–M'89–SM'94) received the Ph.D. degree in electrical engineering from the University of Illinois at Urbana-Champaign (UIUC) in 1989.

His research interests include computational electromagnetics and acoustics and their applications, wave propagation in inhomogeneous media, geophysical subsurface sensing, and inverse problems. He has published more than 100 papers in refereed journals and conference proceedings. He was with the Electromagnetics Laboratory, UIUC, as a Research Assistant from September 1986 to December 1988, and as a Postdoctoral Research Associate from January 1989 to February 1990. He was a Research Scientist and Program Leader with Schlumberger-Doll Research, Ridgefield, CT, from 1990 to 1995. From October 1995 to May 1999 he was a faculty with New Mexico State University, Las Cruces. Since June 1999, he has been an Associate Professor of Electrical Engineering at Duke University, Durham, NC.

Dr. Liu is a member of Phi Kappa Phi, Tau Beta Pi, SEG, a full member of U.S. National Committee of URSI COmmissions B and F, and a Senior Member of IEEE. Currently, he serves as an Associate Editor for IEEE TRANSACTIONS ON GEOSCIENCE AND REMOTE SENSING. He received a Presidential Early Career Award for Scientists and Engineers (PECASE) from the National Science and Technology Council (NSTC) and an Early Career Research Award from the Environmental Protection Agency in 1996, and a CAREER Award from the National Science Foundation in 1997.

Guo-Xin Fan (M'97) received the Ph.D. degree in electrical engineering from Tsinghua University, Beijing, China, in 1995.

From 1985 to 1990, he was engaged in research as a Research Engineer and the Head of a research group on the theory and techniques on subsurface detection at the China Research Institute of Radiowave Propagation, Xinxiang, China. He was in charge of the development of the first practical ground-penetrating radar in China. From September 1995 to August 1997, he was a postdoctoral research fellow in the Electromagnetics Laboratory, Department of Electrical and Computer Engineering, University of Illinois at Urbana-Champaign. From August 1997, he has been a postdoctoral research associate in the Electromagnetics Laboratory, Klipsch School of Electrical and Computer Engineering, New Mexico State University, Las Cruces. His research interests include computational electromagnetics, electromagnetic scattering, slotted-waveguide array antenna, subsurface target detection, and development of ground-penetrating radar.

Dr. Fan was the first winner of a Science and Technology Program Award of the Ministry of Electronics Industry of China in 1991.